Pore geometry and pore-fluid types: Effects on seismic properties of carbonate rocks under a compaction disequilibrium scenario

Gautier Njiekak, Department of Physics, Institute for Geophysical Research, University of Alberta, Canada
njiekak@ualberta.ca
and
Douglas R. Schmitt, Department of Physics, Institute for Geophysical Research, University of Alberta, Canada

Summary

The current paper aims at assessing the influence of the pore geometry and the pore fluid types on the variation of the seismic properties of carbonate samples for the case of a compaction disequilibrium scenario. The main motivation of this study lies in the necessity to extend the experimental basis for the elastic properties of carbonate rocks, which is critical for a better understanding of the relationship between geophysical observables (e.g., seismic velocity) and other measurable rock properties (e.g., porosity and permeability) in carbonate reservoirs.

Ultrasonic measurements of P- and S-waves velocities (Vp and Vs) were conducted on two carbonate samples displaying similar amounts of porosity (θ) but different porosity types: an oolithic limestone (sample OL, θ = 17%) characterized by a grain-supported fabric containing mostly sub-rounded pore spaces and a sucrosic dolomite (sample SD, θ = 15%), the less stiff of the two studied samples, with a porosity dominantly made of intercrystalline pore spaces. The contrast in the velocity variation between the two samples suggests the pore types to be the primary factor controlling the velocity under dry and vacuum conditions.

Experiments under fluid-saturation conditions at a constant differential pressure (difference between the confining and pore-fluid pressure) allowed for the assessment of the effects of porosity type (stiff intergranular pore system vs less stiff intercrystalline pore framework) and of the pore-fluid type (nitrogen vs distilled water) on the variation of the rock elastic properties. The scenario simulated in our study was that of a compaction disequilibrium scenario, i.e., with pore-fluid pressure and confining pressure being incrementally changed at the same rate. A constant differential pressure of 25 MPa was used during the fluid-saturated experiments.

Under nitrogen saturation, regardless of the rock fabric, the effect of the pore-fluid pressure on the variation of Vp and Vs is greater than that of the confining pressure; the bulk density being the primarily factor controlling the variation of Vp and Vs. Under water saturation, sample OL shows no variation of Vp and Vs, which is indicative of changes in velocities being only dependent on the differential pressure. On sample SD, which contains more compliant elements than sample OL, the bulk and shear moduli dominate over the bulk density for the control of the velocity.

Introduction

Because of the extreme porosity variability and the significant textural heterogeneities inherent in carbonates, unlocking rock physics of carbonate reservoirs can be a quite complicated task. Indeed, unlike in silicilastic rocks, bulk porosity and pore-fluids are not the only primary controlling factors in determining the velocity in carbonate rocks, pore geometry (shape and size) can be equally important (e.g., Wang, 1997; Eberli et al., 2003). The many attempts to describe the pore geometry of carbonates have led to the conclusion that a relation exists between the scatter in velocity data and the pore type (e.g., Anselmetti and Eberli, 1997; Eberli et al., 2003); intragranular pores (i.e., moldic and intraframe porosity) generally correlate with significantly higher velocity values than intergranular pores (i.e., interparticle and intercrystalline porosity). Baechle et al., (2008) correlate pore size fractions to velocity data, and show that the percentage of macropores from quantitative digital image analysis of thin sections positively correlates with increasing velocity. The authors also indicate that the fraction of stiff macropores versus soft micropores is responsible for the variation of velocity at any given porosity.

The current paper aims at assessing the influence of the pore geometry and the pore fluid types on the variation of the seismic properties of carbonate samples for the case of a compaction disequilibrium scenario. The main motivation of this study lies in the necessity to extend the experimental basis for the seismic properties of carbonate rocks, which is critical for a better understanding of the relationship between geophysical observables (e.g., seismic velocity) and other measurable rock properties (e.g., porosity and permeability) in carbonate reservoirs.

In our study, two carbonate samples displaying similar amounts of porosity but different porosity types are used to perform the investigations. Nitrogen and water are used one at a time as saturating fluid. This allows for the assessment of the influence of the porosity type and of the pore-fluid type on the variation of the seismic properties of the studied samples. The compaction disequilibrium scenario used in our experiments is simulated by increasing pore-fluid pressure and confining pressure at the same rate and then decreasing them to the initial conditions.

Sample description

An oolitic limestone (sample OL) and a dolomite (sample SD) are the two carbonate rocks investigated in this paper.

Sample OL displays a grain-supported framework with intergrain pore spaces sometimes filled with blocky calcite crystals (Figs. 1a, c, e). The internal structure of the individual grains is often micritized. Calcite is the main mineral of the rock, forming more than 90% of its mineralogical composition. Quartz is the other mineral in the rock. The grain density of sample OL is 2.65 g/cm3. The average grain size is between 0.3 mm and 0.4 mm and the main pore throat size is around 35 µm (Fig. 1g). The rock porosity obtained by means of helium pycnometry is 17 %. The air permeability is lower than 2 mD.

Aside of dolomite that forms more than 90% of the mineralogical composition of sample SD, calcite, quartz and anorthite are the other minerals present in the rock. Loosely packed grains and a generally intercrystalline porosity are the main characteristics of the dolomite fabric (Figs. 1b, d, f). The grain density of sample SD is 2.78 g/cm3. The average grain size is

around 7 µm and the main pore throat size is about 0.7 µm (Fig. 1h). The rock porosity obtained by means of helium pycnometry is 15 %. The air permeability is lower than 2 mD.

Ultrasonic measurements: methodology

Experimental setup and procedure: Ultrasonic measurements were performed by using the pulse transmission technique. The experimental setup included several functional units such as a pressure vessel, a heat tape wrapped around the pressure vessel to control the temperature, a pulse generator, a set of specially constructed transmitting and receiving transducers (resonant frequency = 1 MHz), tanks as pore-fluid sources, independent pumps for regulating confining and pore-fluid pressures and a digital oscilloscope for recording waveforms. More detail on the experimental setup and procedure can be found in Njiekak et al., 2013. The samples were tested dry and fluid-saturated at room temperature; nitrogen and distilled water were the saturating fluids. The length and the diameter of the sample plugs used in the experiments were 4.7 cm and 3.8 cm, respectively.

Testing sequence: The testing sequence consisted of:

(1) Obtaining the P- and S-waveforms with increasing confining pressures (up to 32 MPa), followed by unloading (to 1 MPa), but with the pore space subject to vacuum to provide the properties of the dry rock.

(2) Performing measurements with the pore space saturated with inert nitrogen gas. These tests carried out at constant differential pressure of 25 MPa. This allowed for the simulation of a compaction disequilibrium type mechanism and the assessment of the effective stress variations that could occur in the sample.

(3) Putting the pore space of the tested sample under vacuum for 6–8 h and then repeating the ‘dry’ measurements. This allowed for the assessment of any mechanical change that could have altered the rock ‘dry’ properties.

(5) Finally carrying out the measurements under full saturation with distilled water at constant differential pressure.

For all the dry and saturated measurements, the measurements were taken after incremental pressure change of 1 to 5 MPa during pressurization and/or depressurization cycles. The samples were allowed to equilibrate at constant pressure for about 15 to 20 min prior to acquisition of the waveforms. To reduce random noise effects, the final waveform recorded was a stack of at least 200 traces. Uncertainty in the measured velocities is estimated to be around 0.1% because of errors in the sample length and in the travel time picking for both the calibration and sample measurements.

Ultrasonic measurements: results and interpretations

- Under dry and vacuum conditions (Fig. 2)

On the stiffer sample (sample OL), P- and S-wave velocities (Vp and Vs) increase by up to 2%. The amount of change of Vp and Vs with pressure on sample SD is up to 10%.

As mentioned above, calcite and dolomite are the respective dominant minerals in samples OL and SD, each forming more than 90% of the rock mineralogical composition. However, for the range of confining pressures used in this study, it is rather difficult to assume a direct correlation between known seismic velocities in minerals calcite (Vp = 6500 m/s and Vs ~ 3500 m/s) and dolomite (Vp = 7300 m/s, Vs ~ 4000 m/s; e.g., Wang, 1997; Eberli et al., 2003) and the velocities on the studied dry samples OL and SD. At the highest confining pressure (32 MPa) applied on both dry samples, the dolomite sample (sample SD) has the highest Vs but the lowest Vp. Since Vp and Vs on sample SD are still increasing under the highest confining pressure, it is more appropriate to assume that the rock fabric, and not the type of carbonate minerals, is the primary factor controlling the velocity on the dry samples. As for the effect of the rock fabric on the velocity, since samples OL and SD have almost similar pore volume (17% and 15 %, respectively), we assume that the causes for the differences in the behaviors of Vp and Vs are mainly related to the pore types and less to the bulk porosity. The porosity in sample OL is dominated by sub-rounded pores, which should be less stress sensitive than the intercrystalline pore types displayed by sample SD.

- Under fluid-saturated conditions (Figs 3 and 4)

Under nitrogen saturation: During the nitrogen-saturated experiments, nitrogen turned from gas to a supercritical fluid in the rock pore spaces (Lemmon et al., 2011). This increased the bulk density of the investigated samples but, as suggested by the changes in Vp, the pore space compressibility was less affected. The saturated rock bulk density dominates over the elastic moduli for the control of Vp and Vs on both studied samples. The magnitude of the saturation effect seems to be independent of the rock fabric; Vp and Vs display similar respective amounts of decrease on the two samples.

During the water-saturated experiments, the coupled effect of increasing pore-fluid and confining pressures keeps Vp and Vs constant on sample OL. Conversely, Vp and Vs slightly increase with water saturation on the sample SD suggesting both velocities to be more confining pressure-dependent.

Under water saturation: In our analysis, we are distinguishing two phases for the water-saturated experiments. The first phase (phase 1) corresponds to the initial level of the saturation, i.e., when Pp = 1 MPa and Pc = 26 MPa. The second phase of saturation (phase 2) corresponds to the further stage of the water-saturated experiments, with both Pp and Pc being raised at the same rate from 1 MPa and 26 MPa, respectively, upward and then decreased to the initial conditions. Based on the ‘water-saturated’ velocities measured in this study, the injection of water into the studied samples are assumed to cause the following effects: (i) pore stiffness increase resulting in the increase of the rock bulk modulus, (ii) either shear strengthening (i.e., increase of the dynamic shear modulus) or shear weakening (i.e., decrease of the dynamic shear modulus), and (iii) the increase of the bulk density. The rate at which these effects occurred likely controlled the change in the velocity. The timing of occurrence of water-saturation effects on the two studied samples can be summarized as follows:

- on sample OL, the increase of Vp at the initial stage of the water saturation (phase 1) suggests that the bulk modulus increases faster than the bulk density. The observed drop of

Vs at this stage is due to a faster increase of the bulk density compared to that of the shear modulus. In fact, a 2% increase of the shear modulus has been recorded during the phase 1 of the water saturation. During the phase 2 of the water saturation, the effects of the increase of the elastic moduli and the bulk density cancel each other causing Vp and Vs to remain constant.

- On sample SD, Vp and Vs firstly drop during the phase 1 of the water saturation and then slightly recover during the phase 2. The increased bulk density is the main influential factor controlling the velocity during phase 1, whereas the bulk and shear moduli dominate over the bulk density for the control of Vp and Vs, respectively, during the phase 2. The reason for such a change in the nature of the main influential factor between phase 1 and phase 2 is not well understood yet but could well be related to local flow mechanisms (e.g., Wang and Nur, 1990) that accounts for the effect of pore-scale fluid flow and pressure equilibrium on the elastic moduli (Wang, 1997). Indeed, we can assume that, due to variations in the compressibility of the pores in sample SD, the passing elastic wave caused fluid flow from compliant pores to stiff, less compliant ones. Due to the ultrasonic frequencies used in our study and/or the small size of the dominant pore throat in sample SD (0.7 µm compared to 35 µm in sample OL), water could have required much more time to equilibrate during the passing wave. This then resulted in higher values of Vp and Vs during the phase 2 of the water saturation experiments.

Conclusions

Ultrasonic measurements of P- and S- waves velocities conducted on two carbonate samples at room temperature allowed for the assessment of the effects of the pore geometry and pore-fluid types on the variation of the rock seismic properties. The two carbonate samples have a similar amount of porosity but different dominant pore types; sample OL (porosity: 17%) is an oolithic limestone characterized by a grain-supported fabric containing mostly sub-rounded intergranular pores and sample SD (porosity: 15%), the less stiff of the two studied samples, is a sucrosic dolomite with a fabric consisting of loosely packed grains and a generally intercrystalline porosity. The contrast in the velocity variation between the two samples under dry and vacuum conditions suggests the pore types to be the primary factor controlling the velocity.

From the experiments performed under a constant differential pressure of 25 MPa, with nitrogen and distilled water used one at a time as saturating fluids, following observations have been made:

(i) - For a compaction disequilibrium scenario under nitrogen saturation, with pore-fluid pressure changing incrementally from 1 to 12 MPa and confining pressure changing from 26 to 37 MPa, the saturated rock bulk density dominates over the elastic moduli for the control of the velocity on both samples. Thus, regardless of the rock fabric, the effect of the pore-fluid pressure on the variation of Vp and Vs appears to be greater than that of the confining pressure under nitrogen saturation (with nitrogen turning from gas to a supercritical fluid in the pore spaces during the experiment).

(iii) - For the same compaction disequilibrium scenario under water saturation, P- and S-wave velocities remain constant on the stiffer carbonate rock (sample OL). This is indicative of changes in velocities being only dependent on the differential pressure (= confining pressure

minus pore-fluid pressure). In other terms, the effects of the increased elastic moduli following water saturation are cancelled by the increased bulk density.

On the sample displaying a more compliant pore system (sample SD), the bulk and shear moduli dominate over the bulk density for the control of Vp and Vs, respectively. Local flow mechanisms could have been one of the main factors causing the observed changes of the elastic moduli.

Acknowledgements

The development of the measurement system was supported by NSERC and the Canada Research Chair program. Gautier Njiekak was supported by a research grant from Carbon Management Canada. We thank the Saskatchewan Core Repository for providing us the samples and Randolf S. Kofman for his assistance in the laboratory.

References

Anselmetti, F. S., and G. P. Eberli, 1997, Sonic velocity in carbonate sediments and rocks, in I. Palaz and K. J. Marfurt, eds., Carbonate seismology, SEG Geophysical Developments Series 6, 53–74.

Baechle, G. T., A. Colpaert, G. P. Eberli, and R. J. Weger, 2008, Effects of microporosity on sonic velocity in carbonate rocks: The Leading Edge, 27, 1012–1018.

Eberli, G. P., G. T. Baechle, F. S. Anselmetti, and M. L. Incze, 2003, Factors controlling elastic properties in carbonate sediments and rocks, The Leading Edge, 7, 654–660.

Lemmon, E.W., McLinden, M.O., Friend, D.G., 2011, In: Linstrom, P.J., Mallard, W.G. (Eds.), Thermophysical Properties of Fluid Systems in NIST Chemistry WebBook, NIST Standard Reference Database Number 69, National Institute of Standards and Technology, Gaithersburg MD, 20899, http://webbook.nist.gov (retrieved 2008–2011).

Njiekak, G., Schmitt, D. R., Yam, H. and Kofman, R.S., 2013, CO_2 rock physics as part of the Weyburn-Midale geological storage project, International Journal of Greenhouse Gas Control, 16S, 118-113.

Wang, Z., 1997, Seismic properties of carbonate rocks, in I. Palaz, and K. J. Marfurt, eds., Carbonate Seismology: Geophysical Developments, 6, 29–52.

Wang, Z., and Nur, A., 1990, Dispersion analysis of acoustic velocities in rocks: J. Acoust. Soc. Am., 87, 2384-2395.

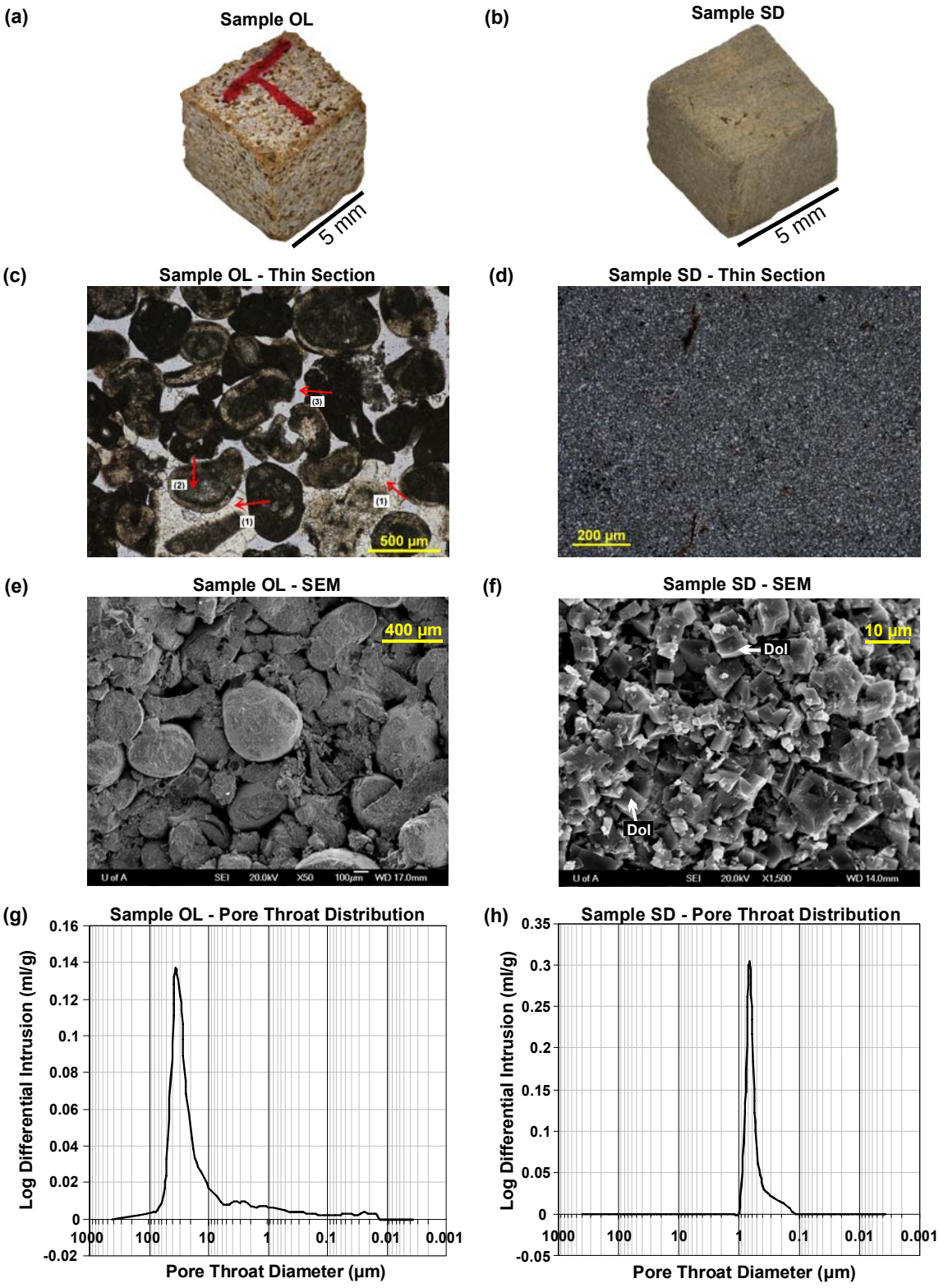

Figure 1: Photo(micro)graphs and pore size distribution of the studied samples. *(a)* and *(b)* Small fragments of sample OL and sample SD; (c) and (*d*) Thin sections (plane-polarized light): (*c*) Note the blocky calcite cement (arrow 1) and the porosity in intergrain space (arrow 3) in sample OL; the internal structure of the allochems are often micritized (arrow 2). Porosity is filled with a grey to blue-dyed epoxy on the thin section. (*d*) Note the loosely packed dolomite crystals from the SEM image. Dol = Dolomite.; (*e*) and *(f)* SEM images; *(g)* and *(h)* Log differential intrusion vs. pore size for the matrix of the two samples. Dominant pore throat sizes are 35 µm and 0.7 µm in samples OL and SD, respectively.

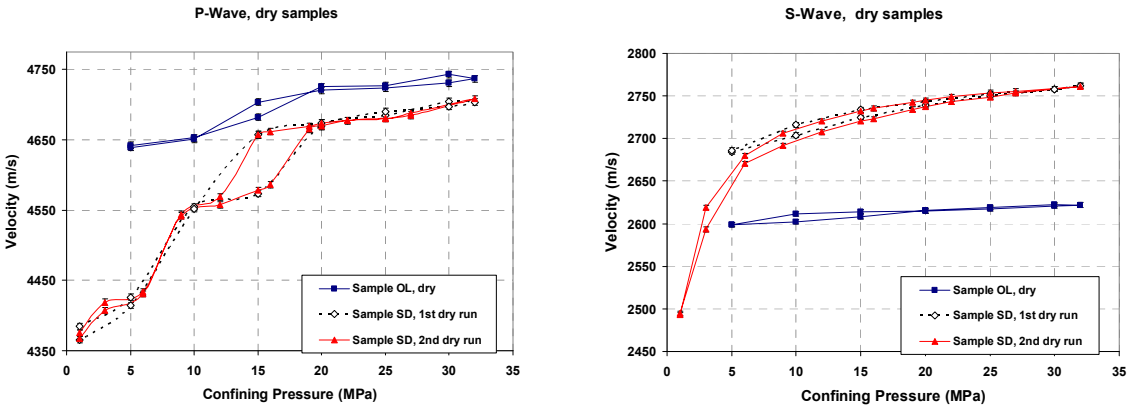

Figure 2: P- and S-waves velocities under dry and vacuum conditions on the studied samples. Note the wide range of variation of the velocities measured on sample SD. For quality control purposes, two 'dry' runs were performed on the less stiff sample (sample SD) to check for any hysteresis effect due to slow recovery; the second run was conducted about 12 hours after the first one. There is a good match between the velocities measured during the two runs**.** Uncertainty in the velocities is around 0.1%.

a)

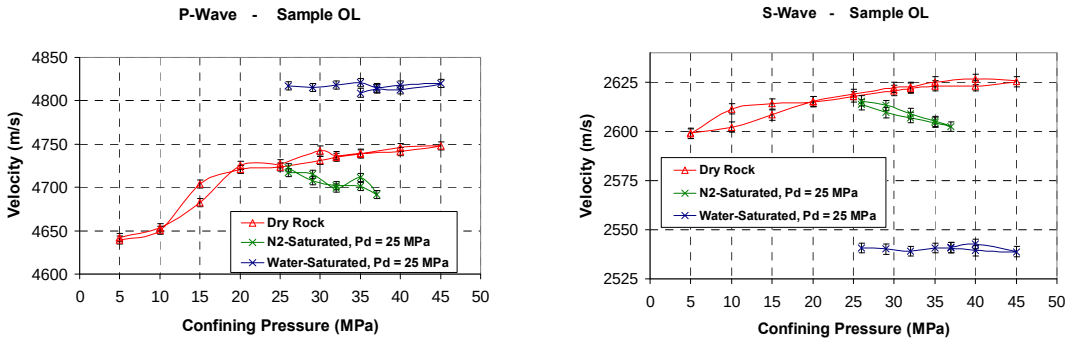

b)

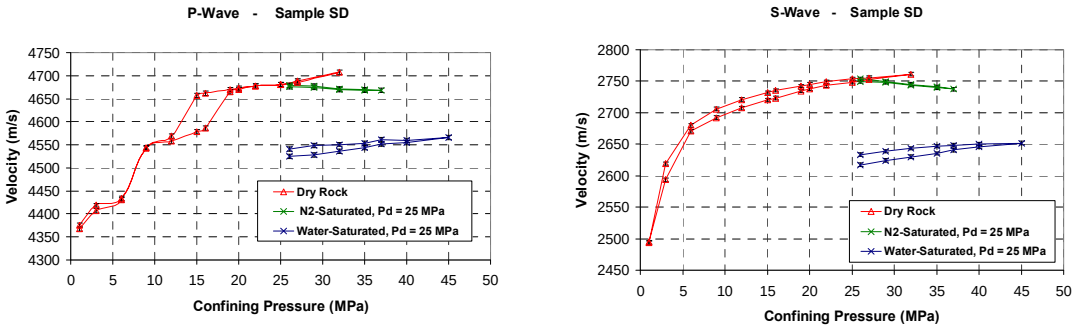

Figure 3: 'Dry' and 'fluid-saturated' velocities on *(a)* sample OL and *(b)* sample SD. Pd = differential pressure.

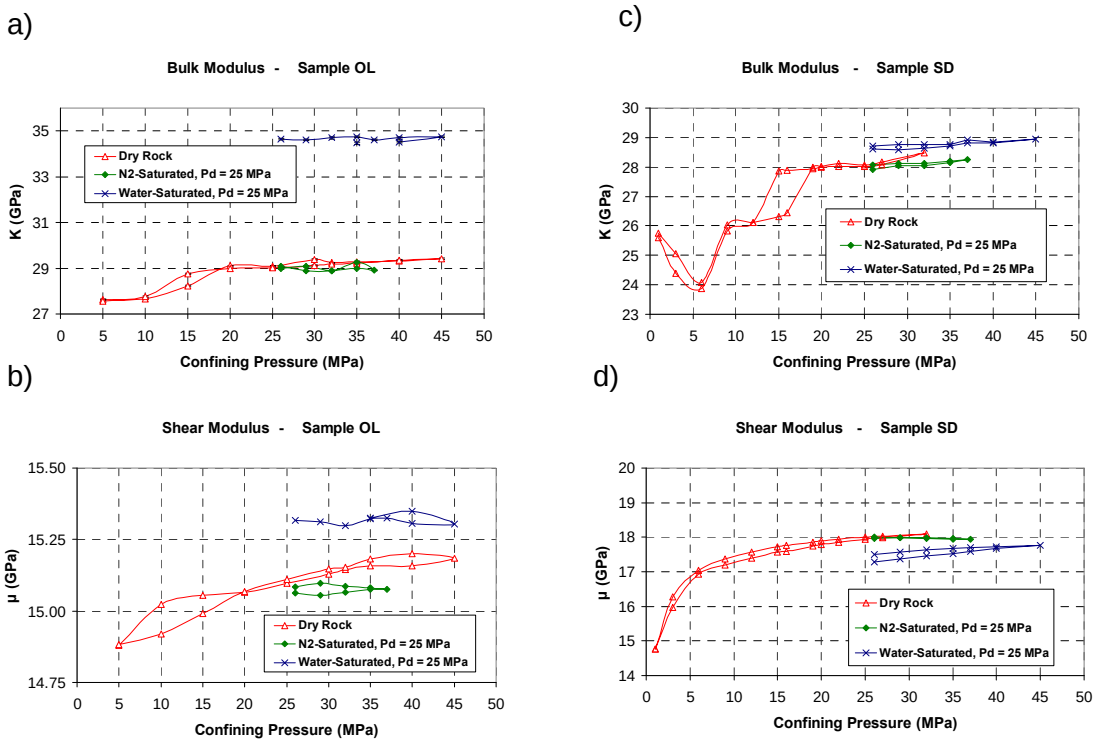

Figure 4: Bulk modulus and shear modulus on *(a) and (b)* sample OL and *(c) and (d)* sample SD for the dry and fluid-saturated conditions. Pd = differential pressure.